AIN SHAMS UNIVERSITY
FACULTY OF ENGINEEING

Vol. 43, No. 1, 31 March, 2008

SCIENTIFIC BULLETIN
Received on :9/2/2008
Accepted on :29/3/2008
PP. :121-138

DESIGN MODEL FOR CIRCULAR BASE PLATES UNDER BENDING MOMENT

M. A. GHAREEB[1], S. A. HEIKAL[2] & M. A. KHEDR[3]

ABSTRACT

The present study aims at examining the behaviour of circular base plate connections under bending moment. An experimental program is developed and tests are performed on twelve pipe specimens with circular base plate and circular anchor bolt pattern. Pipe diameter, base plate diameter, number of anchor bolts and bolt circle diameter are all kept constant throughout the experimental investigation. Base plate thickness and the presence of plate stiffeners are the varied parameters. The specimens are loaded till failure under vertical tip load and failure mechanism is determined. The results of the tests are presented in the paper. The presented experimental data is used in the development of a design model for circular base plates implementing a yield line analysis.

ملخص البحث

البحث يهدف الى دراسه سلوك وصلات الواح ألارتكاز الدائريه تحت تأثير عزوم الانحناء . تم عمل برنـــامج عملـــى لاختبار عدد 12 ماسوره متصل بها الواح أرتكاز يثبت بها عدد من الجوايط على المحيط الـــدائرى. قطـــر الماســـوره وقطر لوح الأرتكاز وعدد جوايط التثبيت وكذلك قطر الجوايط تم تثبيته اثناء الأختبارات. تـــم تغييـــر ســـمك الـــواح الأرتكاز في النوعين الذين تم اختبارهما من الوصلات، نوع به اعصاب تقويه وأخرى بدون. تم عرض النتائج المعمليه واستخدامها فى أستنتاج نموذج تصميمى.

NOTATIONS

A_b	area of bolt cross section
B_{yli}	yield load of the bolt
D_b	diameter of bolts circle
D_i	inner diameter of base plate
$D`_i$	radiuse of plastic hinge circumference
f_y	yield stress
f_{yb}	yield strength of the bolt
M_{cy}	connection yield moment
M_{yl}	yield moment of plate
l_{uv}	the length of yield line $\overline{uv}$ formed between the planes u and v

[1] Arab Steel Fabrication (El Sewedy), 10th of Ramadan City, Industrial Zone 3, Egypt, E-mail: mghareeb@elsewedysteel.com
[2] Department of Structural Engineering, Ain Shams University, Abbasia, Cairo, Egypt,E-mail: samirheikal@hotmail.com
[3] Department of Civil Engineering, Higher Institute of Technology, Benha University Al Ahram Street, Benha, Egypt, E-mail: mkhedr@hotmail.com

P_y	yield load
U_I	internal work generated
U_E	external work generated
U_b	internal work generated through the yieldieng of bolts
U_p	internal work generated through the formation of plastic yield lines
m_p	plastic moment per unit length
t_p	thickness of base plate
T_b	allowable tension strength in bolt
T_{yl}	tension force in bolt calculated using yield line analysis
s	size of fillet weld
k_i	reduction factor to define value of virtual displacement at joint i
θ_{uv}	rotation undergone by the yield line $\overline{uv}$ formed between the planes u and v
δ	assumed virtual displacement
δ_{bi}	virtual displacement of the bolt

1 INTRODUCTION

Circular base or flange plates are widely used in pylons in cable-stayed bridges, telecommunication and lighting structures. Self-supporting latticed towers with pipe or solid round legs usually have a round flange plate, which is subjected mainly to tensile or compressive forces (if eccentricities exist).

Straight and tapered poles on the other hand have circular base plate, which is subjected mainly to bending moment in addition to shear force. Several research works have been done which were devoted to the design of circular base plate under axial load (B. Kato and R. Hirose 1985). However, the behaviour of circular base plates under bending moment has not been studied or at least has not been documented in the published literature.

This paper presents an experimental series of tests performed in Benha University to study the behaviour of circular plates under such loading conditions. The main parameters varied in the tests were the base plate thickness and the presence of stiffeners in the base plate connection. A total of twelve specimens were tested. The specimens were divided into two series: Type N connections for non-stiffened base plate; and Type S connection for stiffened base plate. In both series, circular hollow sections were tested. The twelve specimens were divided into three groups according to their base plate thickness (10, 12 and 16 mm).

This data is very important to help developing an analytical model of the same case of study. Along with the experimental work, a yield line analysis is also presented for the same configurations used in the tests.

The analysis was prepared using the yield line method. A proposed pattern of the non stiffened end plate is presented and analysed. From the analysis, a theoretical value of the yield moment of the base plate is obtained.

2 EXPERIMENTAL WORK: TEST SPECIMENS AND MATERIAL PROPERTIES

2.1 Base Plate and Anchor Bolt Details

The general layout of the base plates is shown in Figure (1) for Type N and Type S connections.

The thickness (t_p) varied from 10 to 16 mm and dimensions (D_i) and (D_b) were kept constant for all the specimens.

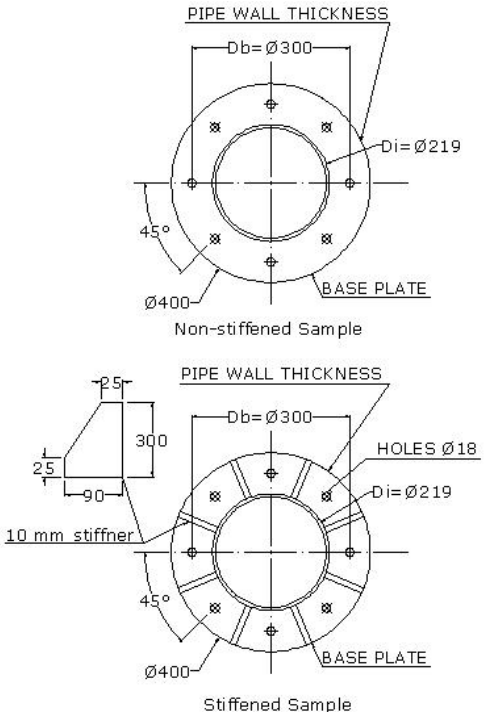

Fig. 1: Base Plate Detail

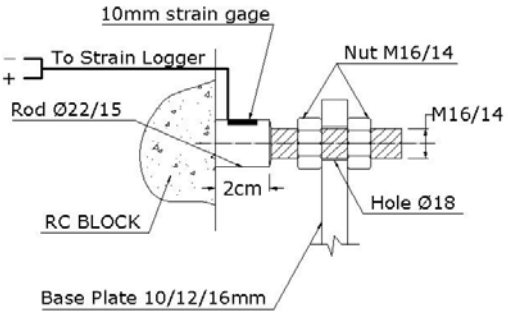

Fig. 2: Anchor Bolt Detail

The anchor bolt assemblies used in the base were black M14 and M16 high strength grade 60 and 52 respectively. For the 10 mm base plate a total of 8 Nos. M14 anchor bolts were used, for the other two categories a set of 8 bolts with M16 anchors were used. The unthreaded shank of the bolt was chosen to be 2 cm for all the specimens in order to suit a 10 mm strain gauge, Figure (2).

2.2 Material Properties of the Anchor Bolt and the Base Plate

For M14 bolts the nominal yield stress was 786 MPa and 437 MPa for the M16. Tensile coupons were taken from the base plates and tested. Table (1) shows the material property of the base plates used in the tests.

Table 1: Material Property of the Base Plates

Specimen	Yield Stress (MPa)	Ultimate Tensile trength (MPa)
10 mm	251	397
12 mm	284	461
16 mm	288	464

2.3. Testing Procedure

Each test consisted of a pipe specimen, welded to a circular base plate, attached to anchor bolts which are embedded in RC block, Figures (3) and (4).

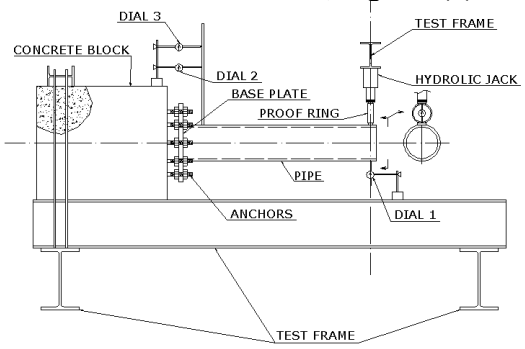

Fig. 3: Test Setup

The specimens were rested on levelling nuts to adjust its horizontality and no grouting between the base plate and the RC block was used, therefore there was no prying force affecting the connection. The specimens were tested by applying load at the tip point of the pipe using a hydraulic jack until failure.

The distance between the loading point and the base plate was kept constant for the twelve tested specimens and equals 930 mm. The load was applied using equal increments of 2.45 kN For each load increment, the strain gauge readings were recorded using a data logger connected to the system. To measure the vertical displacement of the tip, Dial 1 - Figure (3) - was placed on bottom side of the pipe. Dials 2 and 3 were placed to measure the slope of the vertical bar attached to the pipe hence the total rotation of the connection.

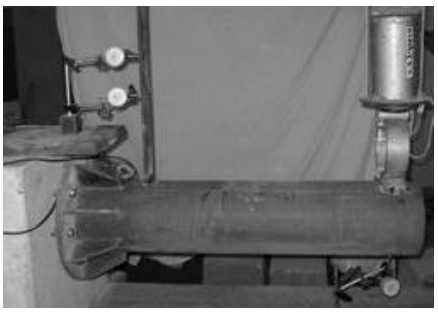

Fig. 4: Stiffened Specimen Being Tested

3 TEST RESULTS AND DISCUSSION:

The twelve specimens were loaded till failure in the test setup shown in Figure (3). The applied load, tip displacement, specimen rotation, pipe strain and anchor bolt strains were all recorded or calculated and are presented in Figs. (5) to (15) and Tables (2) and (3). It should be noted that each tested specimen is given a legend using the following format XX-Y-Z, where XX is the base plate thickness, Y is either N or S for non-stiffened and stiffened specimens respectively and Z is the specimen number in the current XX-Y series.

For example 10-S-2 means: Second stiffened specimen with 10 mm base plate.

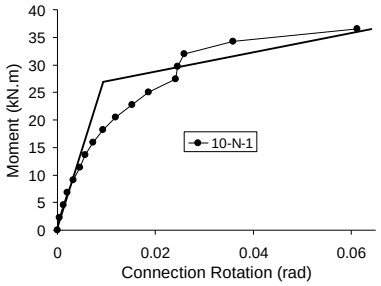

Fig. 5: Moment- Rotation (10-N)

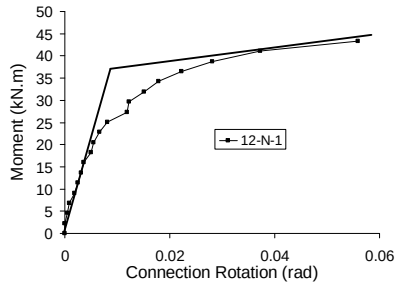

Fig. 6: Moment- Rotation (12-N)

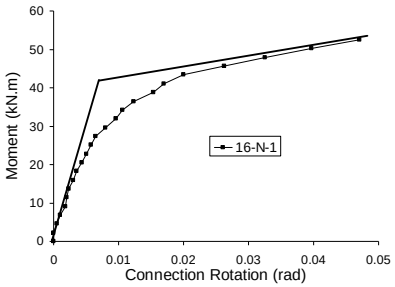

Fig. 7: Moment-Rotation (16-N)

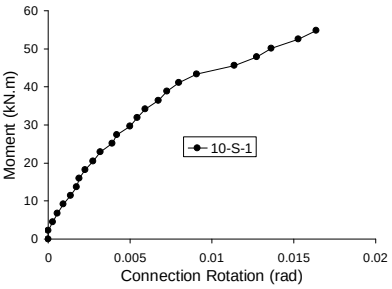

Fig. 8: Moment-Rotation (10-S)

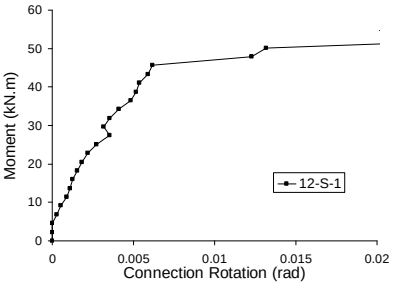

Fig. 9: Moment-Rotation (12-S)

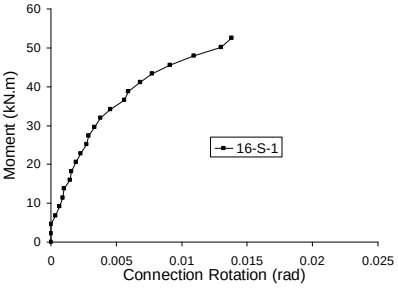

Fig. 10: Moment-Rotation (16-S)

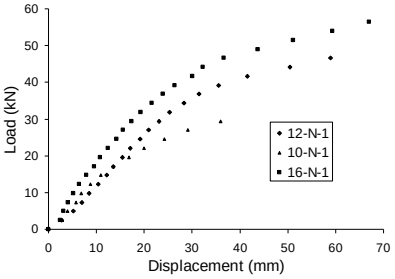

Fig. 11: Load-Displacement Non-Stiffened

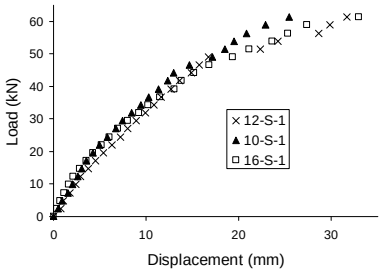

Fig. 12: Load-Displacement, Stiffened

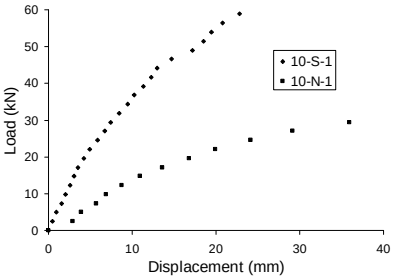

Fig. 13: Load-Disp. Comparison for 10-N&S

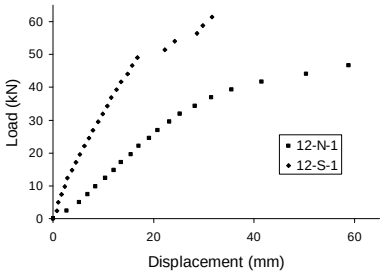

Fig. 14: Load-Disp. Comparison for 12-N&S

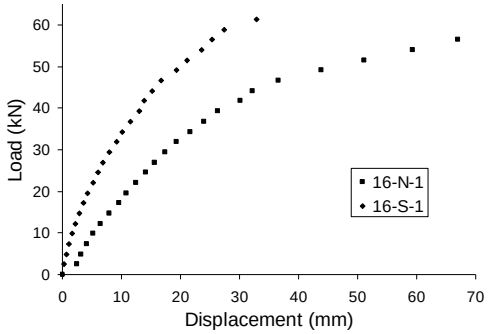

Fig. 15: Load-Disp. Comparison for 16-N&S

Table 2: Yield Load Comparison

Specimen	Yield load (P_y) kN	Yield load (P_{cy}) kN	Ratio
10-N-1	18.63	22.32	1.19
12-N-2	29.42	30.66	1.04
16-N-2	31.87	35.2	1.1

Table 3: Load – Displacement Slope Comparison

Specimen	Slope (N Specimens) kN/mm	Slope (S Specimens) kN/mm	Ratio
10-N-1	128.2	462.96	3.611
12-N-2	128.67	400	3.1
16-N-2	212.76	528.17	2.48

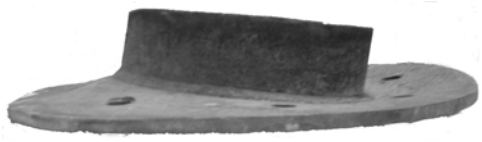

Fig. 16: Deformed Shape of the Base Plate

Fig. 17: Bolt Fracture in Stiffened Specimen

Fig. 18: Nut Slippage

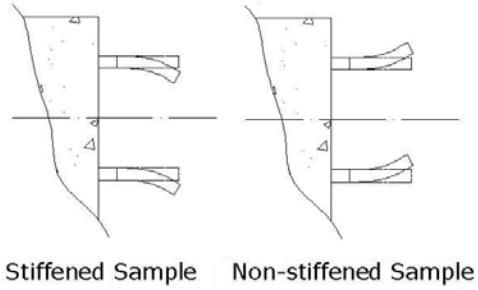

Fig. 19: Deformed Shape of the Bolts

3.1 Description of failure modes

Several failure modes were observed due to the presence of different conditions associated with each tested specimen. The following outlines the main observations:

A- For the non-stiffened specimens, the normal failure mode took place after the base plate started to experience inelastic behaviour, see Figure (16).

B- In the case of stiffened specimens, the failure modes have changed from base plate failure to two other forms as described below:
   a. Failure in the shaft of the specimen
   b. Fracture of the upper bolt carrying the highest tension force, see Figure (17)

C- Pre mature failures have also been experienced and corrected such as:
   a. Bond failure between anchor bolts and the concrete block, specimen 10, 12&16-S-2.
   b. Nut slippage due to manufacturing defects, see Figure (18), specimen 10&12-N-2 and 12&16-S-1.
   c. Excessive local deformation in the pipe underneath the point of load application, specimen 10-S-1

3.2 Analysis of the Results and Observations:

Studying the results collected from the tests of the twelve specimens, the following observations are made:

1. For the non-stiffened specimens, two important values were studied; the first value is the yield load (P_y) which is obtained from the load – displacement graphs by determining the value of the load that created a longer displacement step than its predecessor. The other value is the yield load (P_{cy}) which is obtained form the experimental connection yield moment (M_{cy}). The (M_{cy}) value is defined as the intersection of the initial stiffness and the strain hardening stiffness as shown in Figures (5, 6 & 7). The importance of this comparison is to verify that the displacement of the tip point caused by the yield of the connection and not by premature failures. This comparison is also important to verify the experimental (M_{cy}) value in order to use it in classifying the connection rigidity.
2. Following the Bjorhovde classification scheme, the $\overline{m}-\overline{\theta}$ curves for the non-stiffened specimens were plotted as shown in Figure (20). In this Figure, (θ_c) is the rotation of the connection relative to the attached beam, (M_p) is the plastic moment capacity of the beam cross section, d is the beam depth and (EI_b) is flexural rigidity of the beam section. From this figure one can state that, according to stiffness, the 10mm specimen can be classified as flexible while the 12 and 16mm specimens can be classified as semi-rigid.

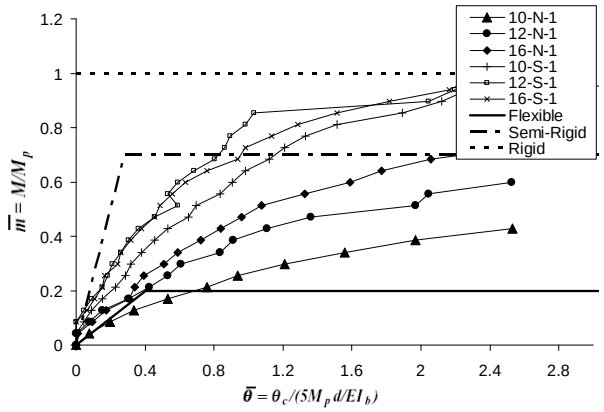

Fig. 20: N Specimen Connection Classification

3. It is obvious that adding stiffeners to the specimens increased the rigidity of the connection and reduced the displacement of the tip point. Table (3) shows comparison between the slope of the N and S specimens with an average ratio of 3.1.
4. From Figure (12) it is noticed that the load deflection curves of the three stiffened specimens are almost similar. This is due to the fact that the presence of the stiffeners contributed more to the rigidity of the connection than the contribution of the base plate thickness to its rigidity.

5. An important difference between the stiffened and the non-stiffened specimen is the behaviour of anchor bolts in the plastic stage. Figure (19) shows the two deformation patterns of the anchor bolts in both cases. For the N specimens, the anchor bolts in the tension zone tend to bend outward while the anchor bolts in the compression zone tend to bend inward, Figure (21). However, in case of the S specimens all the anchors tend to bend downward.
6. The observation regarding the relation between the thickness of the base plate and the rigidity of the connection for the non-stiffened specimens is valid for connections with the ratio of bolt circle diameter (D_V) to pipe diameter (D_i) less than or equal 1.5.

$$\frac{D_v}{D_i} \leq 1.5 \qquad (1)$$

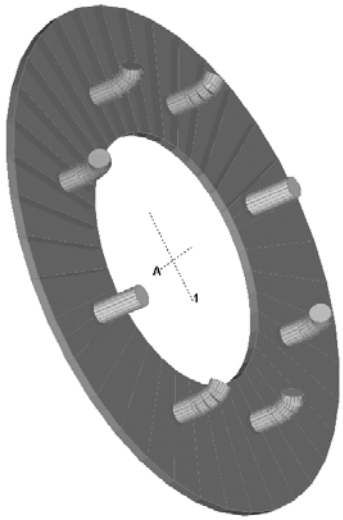

Fig. 21: 3D View Showing the Deformed Shape of Bolts in the N Specimens.

7. For the N specimens during the early stage of loading, the three upper bolts underwent a positive strain due to the tension force. After the base plate started its inelastic behaviour, the strain readings became to show negative sign, especially on the first bolt. This is due to the plate pushing the bolts upward. As a result, the uppermost bolt is acted upon by a combination of tension force and bending moment created by the coupling of the two nuts and deformed shape of the plate. Figure (22) shows the strain readings of the uppermost bolt in specimen 10-N. For the stiffened specimens, the recorded strains of the bolts were higher than that of the non stiffened specimens. Because there was no deformation in the base plate and no coupling around the bolts to force them to undergo negative strain, the strain readings for the S specimens was liner. Figure (23) shows strain readings for specimen 16-S bolt.

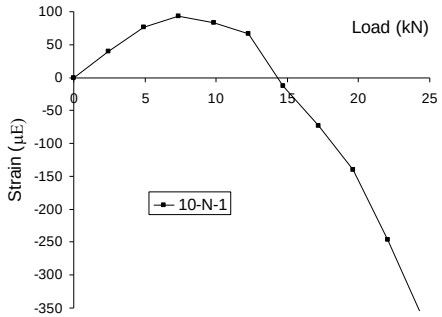

Fig. 22: Typical Strain in Top Bolt (Flexible Connection)

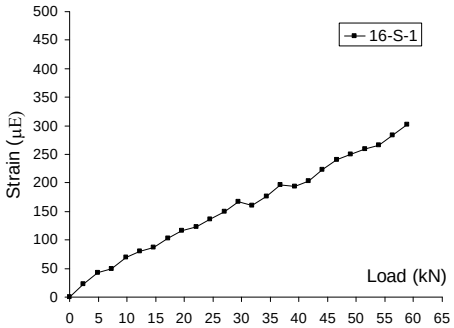

Fig. 23: Typical Strain in Top Bolt (Rigid Connection)

4 YIELD LINE ANALYSIS

Yield line analysis is used to predict the yield moment of the Base plate by studying its shape of failure. In this paper, the methodology used to predict the ultimate moment that can be carried by the plate is discussed briefly. The results of the analysis are presented in a simple form along with the results obtained from the experimental study. It should be noted that the yield line analysis was carried out for the connections without stiffeners (the N specimens).

4.1 Yield Line Pattern

The proposed yield line pattern for the base plate is shown in Figure (24) where three distinct zones are presented.

The grey zone (A) represents the area between bolts circumference and the edge of the base plate. This zone experienced no displacement and remained horizontal. The hatched zone (B) represents the lower part of the area between bolts circumference and the pipe, this part of the base plate performed downward displacement due to the action of the compression force. The white zone (C) represents the part of the base plate performed displacement in the opposite direction of the shaded area due to the action of the tension force.

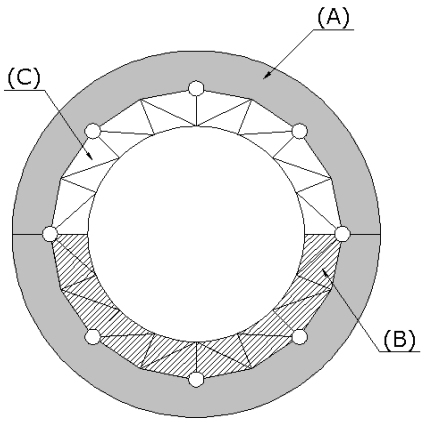

Fig. 24: Proposed Yield Line Pattern

4.2 Analysis of the Deformed Shape:

The virtual internal work (U_I) and virtual external work (U_E) are calculated by introducing a virtual displacement (δ) to the tension area of the base plate of the connection and then determining the internal work generated due to that displacement. The internal work (U_I) is the sum of the work generated through the formation of plastic yield lines (U_p) and yielding of the bolts (U_b),

$$U_I = U_p + U_b \qquad (2)$$

The internal work generated through the formation of yield lines in the end plate is expressed as

$$U_p = (\sum \theta_{uv} \cdot l_{uv}) \cdot m_P \qquad (3)$$

Where m_p is the full plastic moment of the base plate per unit length.

$$m_p = \frac{1}{4} \cdot t_p^2 \cdot f_y \qquad (4)$$

(θ_{uv})is the rotation undergone by the yield line $\overline{uv}$ (formed between the planes u and v), and l_{uv} is the length of the corresponding yield line.

As the yield line patterns developed in the base plate are often complex, the analysis will be simplified by expressing the yield line rotations and lengths in terms of there x and y components.

Hence the work generated in the base plate is expressed in component-wise as

$$U_p = (\sum \theta_{xuv} \cdot l_{xuv} + \sum \theta_{yuv} \cdot l_{yuv}) \cdot m_P \qquad (5)$$

Where l_{xuv} and l_{yuv} are the projections of the yield line $\overline{uv}$ onto the x and y axes, respectively, and the rotations θ_{xuv} and θ_{yuv} are correspondingly defined.

The internal work generated by the bolts is defined as the product of the imposed virtual displacement of the bolt (δ_{bi}), and the yield load of the bolt (B_{yIi}).

$$U_b = \sum B_{yli} \cdot \delta_{bi} \qquad (6)$$

Similarly, the external work is defined in terms of the applied moment as

$$U_E = M_{yl} \cdot \frac{\delta}{2D_i'} \qquad (7)$$

The applied moment to cause plastic collapse of the connection (M_{yl}) is then determined by equating the external work (Equation 7) and the internal work (sum of Equations 5 and 6). Figure (25) shows a simplified 3D segment of the proposed collapse mechanism. Figure (26) shows plan view of one quarter of the base plate divided into intersecting planes 1 to 10.

The maximum displacement is assumed to be (δ) located at joint ($j1$) and ($-\delta$) at the joint located opposite side from joint ($j1$) at the compression side of the flange. In order to form the shape of the mechanism, the flange surface smoothly lean to the compression area through the reduction of the displacement value at each joint by a factor assumed to be (k_i). Therefore the value of the displacement at joint ($j2$) is ($k_1\,\delta$). Using the same concept, the value of displacement at ($j3$) is ($k_2\,\delta$) and at joint ($j5$) the displacement is expected to be zero since this joint lies on the neutral axis of the base plate. In Figure (26), (D_b) is the bolt circle diameter while (D_i) is the inner diameter of the base plate. The plastic hinge is assumed to occur at the centre of the fillet, and the equivalent radius is assumed to be the sum of the pipe outer radius plus half of the fillet size.

$$D_i^{`} = D_i + \frac{s}{2} \qquad (8)$$

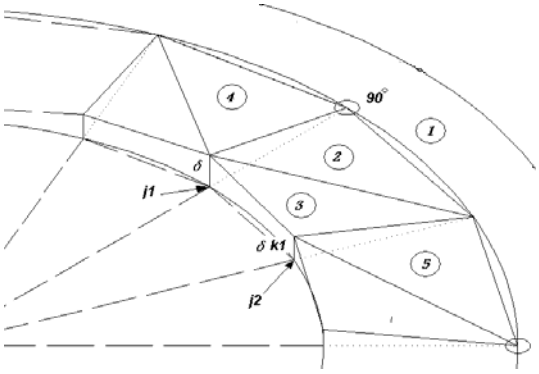

Fig. 25: Simplified 3D View Sketch of Deformed Plate

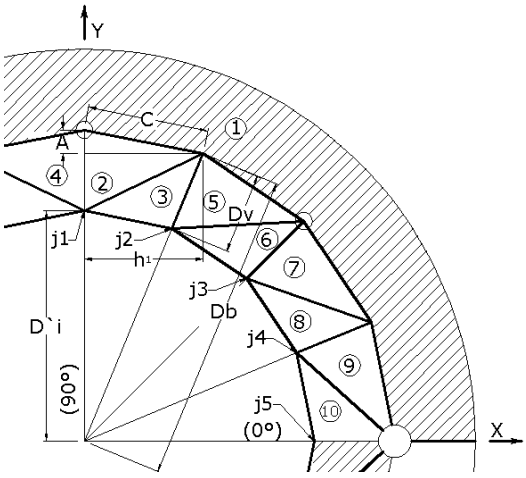

Fig. 26: Simplified Plan View of Deformed Plate

The portion of the base plate analyzed contains planes 1,2,3,4 & 5, which are the basic five planes. These planes are repeated along the pattern in addition to plane 1. Table (4) shows the angels components between each plane, the length of the yield line projection in each angel direction and the related work generated by that line. The values shown are for yield lines between planes (1&2), (2&4), (2&3) and (3&5). Using the symmetry of the pattern, the other angels between the rest of the inclined planes can be obtained by replacing each (δ) with ($k_i\ \delta$) and each (k_i) with (k_{i+1}). For example, to obtain the value of the work generated through the formation of plastic yield line 1-5, the same values obtained for yield line 1-2 can be used but after replacing each (δ) with ($k_1\ \delta$). Same formula can be used for line 7-8 but with using the same formula obtained for line 2-3 after replacing each (δ) with ($k_3\ \delta$) and each (k_1) with (k_4).

The internal work generated (U_{puv}) obtained is for one quarter of the plate. Therefore the work generated for the whole plate is 4 times what is obtained in the table except for the work generated by yield line between plane 2&4 (U_{p24}).

This yield line is repeated only 2 times in the pattern unlike the other yield lines. The value of the internal energy performed can be calculated by assuming the value of (k_i) for each joint and by neglecting the energy performed by the bolts since the strain gage readings for the upper most bolts during the test for the connections classified as flexible was minor.

Therefore this assumption is considered valid for the flexible connections since the base plate is affected more by the applied forces than the bolts.

Table 4: Work Generated Through the Formation of Plastic Yield Lines (U_p): Planes 1 to 5

Yield line	θ_{xuv}	θ_{yuv}	ℓ_{xuv}	ℓ_{yuv}	U_{puv}
1-2	$\frac{\delta}{D_v}$	$\frac{\delta}{D_v}\tan 11.25$	A	h_1	$\frac{\delta}{D_v}(A+h_1\tan 11.25)m_p$
2-4	0	$\frac{2\delta A}{h_1 D_v}$	0	D_v	$\frac{2\delta(1-\cos 22.5)}{\sin 22.5}m_p$
2-3	$\frac{\delta D_b(1-k_1)}{D_v D_i^{`}}$	$\frac{\delta(1-k_1)(D_v-A)}{D_v D_i^{`}\sin 22.5}$	h_1	D_v-A	$\frac{\delta(1-k_1)}{D_v D_i^{`}}(D_b h_1+\frac{(D_v-A)^2}{\sin 22.5})m_p$
3-5	$\frac{\delta x_{35}}{0.146 D_v D_i^{`}}$	$\frac{\delta y_{35}}{0.146 D_v D_i^{`}}$	$D_v sin22.5$	$D_v cos22.5$	$\frac{\delta}{0.146 D_i^{`}}(x_{35}\sin 22.5+y_{35}\cos 22.5)m_p$

Where:

$$X_{35}=(0.146D_b(k_1-1)+D_i^{`}(0.146-0.124k_1) \quad (9)$$

$$Y_{35}=(D_i^{`}(0.354-0.3k_1)-0.354D_b(1-k_1) \quad (10)$$

Table (5) shows the value of the predicted yield moment (M_{yl}) for the three non-stiffened specimens which is calculated using Equation (11) by equating the external work and the internal work calculated from table (4).

In the same table, the experimental (M_{cy}) is presented and the ratio of the predicted to the actual Moment is calculated.

$$M_{yl} = 2D_i' \frac{U_I}{\delta} \qquad (11)$$

From the results shown in table (5), it is noticed that the assumption of neglecting the energy performed by the bolts is not valid for the 16-N specimen. This is because of the extra rigidity added to the connection by the plate thickness.

Table 5: Predicted M_{yl} for non-Stiffened specimens compared with experimental M_{cy}

Specimen	Predicted M_{yl} (kN.m)	Experimental M_{cy} (kN.m)	Ratio
10-N	24.5	24	1.02
12-N	39.7	36	1.1
16-N	62.7	40	1.56

4.3 Connection Strength Limitation

Certain limitations for the above design model should be considered before using it in order to have accurate results. Designers should calculate the allowable tensile strength of the uppermost anchor bolt (T_b) and compare it with the tension force caused by the yield of the plate (T_{yl})

$$T_{yl} < T_b \qquad (12)$$

The allowable tensile strength of the uppermost anchor bolt (T_{bl}) can be calculated by multiplying the area of the bolt into a ratio of the yield strength of the bolt material recommended here to be 60%.

$$T_b = A_b 0.6 f_{yb} \qquad (13)$$

5 CONCLUSIONS

5.1 Non-Stiffened Specimens

- For all the non-stiffened specimens, the yield line has formed between the pipe body and the anchor bolts leading to a helical shape of the base plate.
- For the N specimens, it is noticed that increasing the thickness of the base plate from 10 mm to 12 mm has increased the stiffness of the connection 100%.
- It was found that the rotation of the pipe body can be neglected and the rotation of the connection can be considered as the base plate Rotation combined with the rotation of the anchor bolts.

- It is recommended to use minimum 16 mm thickness of base plate to convert the type of connection from flexible to semi-rigid. Increasing the thickness from 12 mm to 16 mm redistributed the axial force on the anchors which lead to increasing the stress on the uppermost bolt and increased the contribution of the energy performed by the bolts to the energy required for the connection to yield.
- Because the 10-N & 12-N specimens found to be flexible, the assumption of neglecting the internal work generated by the bolts was valid and leaded to good results when compared to experimental results while the same assumption was not valid for the 16-N specimen since the internal work generated by the bolts was higher to be neglected.
- Therefore it is recommended to use the design model obtained from the yield line analysis for flexible connections only. If it is used for rigid connection, the internal energy created by the bolts should not be neglected.

5.2 Stiffened Specimens

For stiffened specimens, no yield occurred in the base plate. The stiffeners welded to the base plate prevented the deformation occurred in the same plates without adding stiffeners.

The initial slope of the load-displacement relationship of the stiffened to the non-stiffened specimens, Figures (13,14&15), indicates that adding stiffeners to the 10 mm specimen converted the connection type from flexible to rigid. For the 16 mm specimen, the effect was not as dramatic however 250% increase in the stiffness of the connection was observed.

6 REFERENCES

[1] Kato, B. and Hirose, R. (1985). "Bolted Tension Flanges Joining Circular Hollow Sections", *Journal of Construct Steel Research*, 5, 79-101

[2] Kato, B., and Mukai, A. (1985). "Bolted Tension Flanges Joining Square Hollow Section Members", *Journal of Construction Steel Research*, 5, 163-177.

[3] Wheeler, A., Clarke, M. and Hancock, G. (2003). "Design Model for Bolted Moment End Plate Connections Joining Rectangular Hollow Sections Using Eight Bolts" *Research Report*, No. R827, Department of Civil Engineering, The University of Sydney, Australia.

[4] Wheeler, A. T., Clarke, M. J., Hancock, G. J., and Murray, T. M. (1998). "Design Model for Bolted Moment End Plate Connections Joining Rectangular Hollow Sections", *Journal of Structural Engineering, ASCE*, 124(2), 164–173.

[5] Wheeler, A. T., Clarke, M. J., Hancock, G. J. and Murray, T. M. (1997). "Design Model for Bolted Moment End Plate Connections Joining

Rectangular Hollow Sections", Research Report, No. R745, Department of Civil Engineering, The University of Sydney, Australia.
[6] Bjorhovde, R., Brozzetti, J. and Colson, A. (1990). A Classification System for Beam to Column Connections, *Journal of Structural Engineering*, *ASCE*, 116(11), 3059-76.
[7] Wheeler, A. T., Clarke, M. J., and Hancock, G. J. (1997). "Bending Tests of Bolted End Plate Connections in Cold Formed Rectangular Hollow Sections", *Research Report*, No. R736, Department of Civil Engineering, The University of Sydney, Australia.
[8] Hag-Elsafi, O., Alampalli, S., and Owens, F. (2001). "New Procedure for Design of End Plates and Base Plates of Cantilevered Traffic Support Structures", *Journal of Structural Engineering, ASCE*. 127(10), 1153-63.
[9] Schaumann, P., and Seidel, M. "Failure Analyses of Bolted Steel Flanges". Institute for Steel Construction, The University of Hanover.
[10] Ghareeb, M., Heikal, S., and Khedr, M. (2007). "A Study in the Behaviour of Circular Base Plates Under Bending Moment". Proceedings, 12th International Conference for Structural and Geotechnical Engineering (ICSGE) 1190-1198.
[11] Kukreti, A. R., Ghassemieh, M., and Murray, T. M., (1990). "Behaviour and Design of Large-Capacity Moment End Plates", *Journal of Structural Engineering*, *ASCE*, 116(3), 809–828.
[12] Cook, R. A., Bobo B. J., and Ansley H. M. (2001). "Design Guidelines for Annular Base Plates", *Research Report*, No. 716, Department of Civil & Costal Engineering, The University of Florida.